Equine Veterinary Journal

Equine Veterinary Journal ISSN 0425-1644
DOI: 10.1111/evj.12845

Biochemical and biomechanical characterisation of equine cervical facet joint cartilage

S. A. O'LEARY[†,1], J. L. WHITE[†,1], J. C. HU[†] and K. A. ATHANASIOU*[†‡]

[†]Department of Biomedical Engineering, University of California, Davis, California, USA
[‡]Department of Biomedical Engineering, University of California, Irvine, California, USA.

*Correspondence email: athens@uci.edu; Received: 21.05.17; Accepted: 30.03.18

Summary

Background: The equine cervical facet joint is a site of significant pathology. Located bilaterally on the dorsal spine, these diarthrodial joints work in conjunction with the intervertebral disc to facilitate appropriate spinal motion. Despite the high prevalence of pathology in this joint, the facet joint is understudied and thus lacking in viable treatment options.
Objective: The goal of this study was to characterise equine facet joint cartilage and provide a comprehensive database describing the morphological, histological, biochemical and biomechanical properties of this tissue.
Study design: Descriptive cadaver studies.
Methods: A total of 132 facet joint surfaces were harvested from the cervical spines of six skeletally mature horses (11 surfaces per animal) for compiling biomechanical and biochemical properties of hyaline cartilage of the equine cervical facet joints. Gross morphometric measurements and histological staining were performed on facet joint cartilage. Creep indentation and uniaxial strain-to-failure testing were used to determine the biomechanical compressive and tensile properties. Biochemical assays included quantification of total collagen, sulfated glycosaminoglycan and DNA content.
Results: The facet joint surfaces were ovoid in shape with a flat articular surface. Histological analyses highlighted structures akin to articular cartilage of other synovial joints. In general, biomechanical and biochemical properties did not differ significantly between the inferior and superior joint surfaces as well as among spinal levels. Interestingly, compressive and tensile properties of cervical facet articular cartilage were lower than those of articular cartilage from other previously characterised equine joints. Removal of the superficial zone reduced the tissue's tensile strength, suggesting that this zone is important for the tensile integrity of the tissue.
Main limitations: Facet surfaces were sampled at a single, central location and do not capture the potential topographic variation in cartilage properties.
Conclusions: This is the first study to report the properties of equine cervical facet joint cartilage and may serve as the foundation for the development of future tissue-engineered replacements as well as other treatment strategies.

Keywords: horse; facet joint; articular cartilage; tissue engineering; mechanical properties; characterisation

Introduction

The equine cervical spine is a highly complex structure known to be vulnerable to the development of disease. The facet joints, also referred to as articular process joints, are positioned dorsally at the cranial and caudal margin of each vertebral arch, with the exception of the C1–C2 articulation. In general, these joints facilitate motion and bear spinal loads in conjunction with the intervertebral discs [1]. The function of these joints is facilitated by a layer of hyaline articular cartilage.

Damage to facet joints can result in clinical signs such as decreased range of motion, as well as forelimb lameness and ataxia [2]. Underlying factors of such clinical signs include developmental abnormalities, such as osteochondrosis [3,4], as well as osteoarthritis [5–8]. Radiographic changes consistent with facet osteoarthritis include joint space narrowing as a result of cartilage degeneration, the development of periarticular osteophytes, widening of the joint space or narrowing of the intervertebral foramina [6]. Although robust epidemiological data are lacking, it has been reported that approximately 50% of horses exhibit degenerative changes of the facet joint at spinal level C6/C7 [5]. Supporting this estimation, in a recent study of 100 skeletally mature horses, radiographic changes consistent with osteoarthritis were found in 38 and 50% of horses at spinal levels C5/C6 and C6/C7 respectively [7].

Unfortunately, treatments available for cervical facet osteochondrosis and osteoarthritis are lacking and largely limited to rest, NSAIDs and intra-articular corticosteroids [2]. Cartilage tissue engineering offers a potential solution for regeneration of damaged facet surfaces that have been shown to be accessible via an arthroscopic approach [9]. Restoration of the articular surface could preclude the progressive bone remodelling that can result from damage to the articular surface and ultimately leads to loss of joint function [10,11]. To tissue engineer facet cartilage, a thorough characterisation must first be conducted to establish design and verification criteria. Unfortunately, there are no existing studies characterising the properties of native equine cartilage of the facet joint. There were two objectives for this study. The first objective was to report morphological and histological characteristics of facet joint articular cartilage. The second objective was to quantify biomechanical and biochemical properties of facet joint articular cartilage across all cervical spinal levels and surfaces. The aim of this study was to provide values to serve as design criteria for therapeutics, as well as yield fundamental knowledge for this often pathological joint.

Material and methods

Specimen preparation

A diagram outlining the sample processing protocol is given in Figure 1. Facet joint cartilage was extracted from the cervical spine of six horses. The horses ranged in age from 4 to 10 years old and were of various breeds, including Quarter horses, Thoroughbreds and Warmbloods. The sample size of n = 6 animals was chosen based on a power analysis using aggregate modulus as an overriding factor. Standard deviation was approximated at 20% based on characterisation of lumbar facet joints in

[1]Joint first authors.

other species [12]. A power of 80% and an α of 0.05 were selected, which yielded a sample size of six animals to detect a biological variability of 25% or greater. The cervical spine was first separated from the skull and the thoracic spine using a bone saw. The skeleton was then cleaned, and the ligaments, muscles and fatty tissues were removed. Using a band saw, the spine was cut in half longitudinally. The intervertebral disc and facet joint capsules were carefully severed at each of the six facet joint levels (C2/C3, C3/C4, C4/C5, C5/C6, C6/C7, C7/T1) using a scalpel, allowing the motion segments to be easily disarticulated. A macroscopic inspection of the cartilage was performed and horses whose cartilage showed signs of OA were removed from the study (from the eight horses examined, two were removed). Photographs of each facet joint surface were taken and ImageJ software was used to measure the width (widest part of the facet joint surface) and the length (longest part of the facet joint surface) of each surface (Fig 2). Following gross inspection, a 6-mm diameter biopsy punch, in combination with a scalpel, was used to remove two samples of cartilage from the bone. The cartilage was consistently harvested from the central region of the articulating surface. In addition, a small piece of cartilage (approximately 10 mg) was removed, weighed (wet weight) and stored at −20°C for biochemical analyses. The 6-mm cartilage samples were wrapped in a gauze soaked in PBS-containing protease inhibitors 10 mmol/L *N*-ethylmaleimide and 1 mmol/L phenylmethylsufonyl fluoride (Sigma[a]) and stored at −20°C until mechanical testing. This process was repeated for each of the six horses; however, considering the bilateral nature of the facet joints' position on the spine, cartilage was harvested from alternate sides of the spine that is three horses had their cartilage removed from the left side and three from the right side. For mechanical testing, samples were thawed for 1 h in PBS, and one sample was used for compression indentation testing while the other was used for tensile testing. For histology, the facet joints of one horse were separated from the vertebral column using a band saw, rinsed and fixed in 10% buffered formalin.

Compression indentation testing

A compression indentation apparatus [13] was used to assess creep and recovery deformation of cervical facet cartilage. Following thawing, a 3-mm diameter punch of tissue was removed from the 6-mm specimen and was photographed. Digital measuring tools (Image J) were used to determine the thickness of hyaline articular cartilage in the sample, and the sample was glued to the base of a cylindrical sample holder. A 0.9-mm flat-ended, porous indenter tip was then programmed

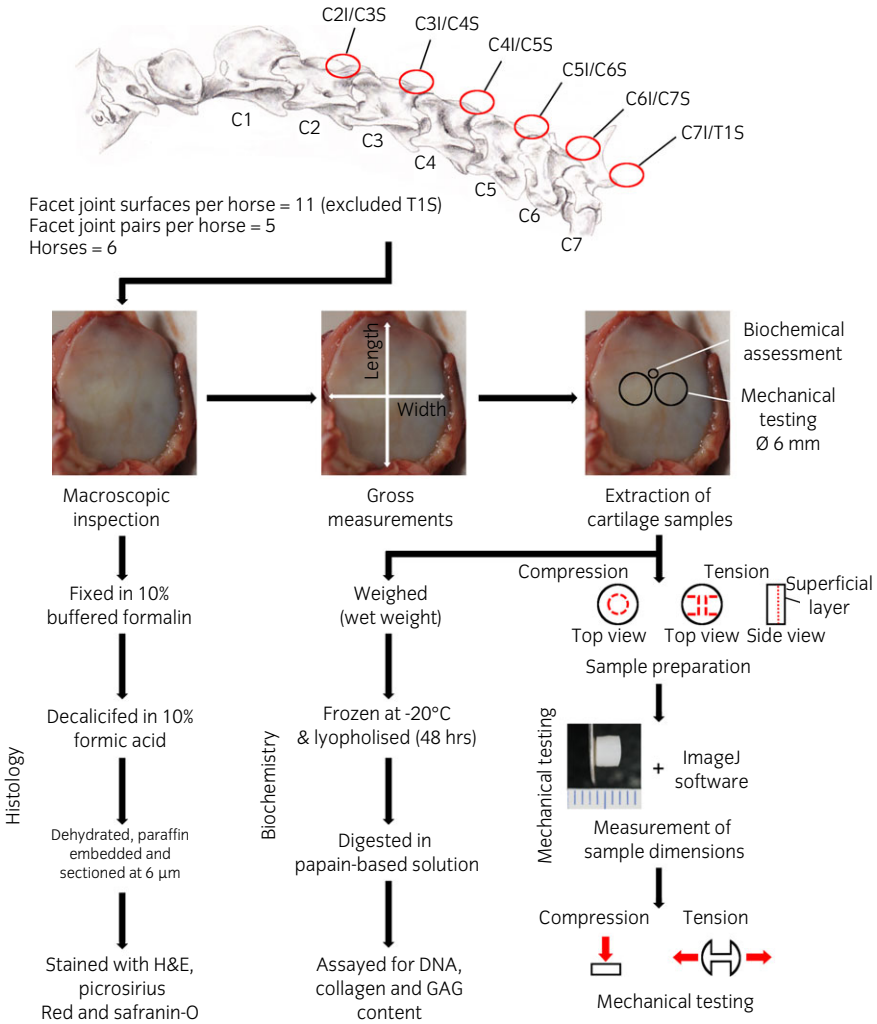

Fig 1: Sample preparation protocol for harvesting test specimens and gross morphometric data. Cervical facet joint locations are denoted with red circles and labelled according to spinal level for example, facet joint C2I(inferior)/C3S(superior) is located at spinal level C2/C3. Upon disarticulation of each cervical facet joint, macroscopic inspection was performed for each joint surface and images were taken for gross measurement analysis. Samples were collected for histology, biochemistry and mechanical testing, and subsequently processed and analysed accordingly. In the mechanical testing diagram, red dashed lines represent where samples were cut to generate testing specimens of the appropriate shape and size. The red arrows indicate the direction of applied force during the mechanical testing modalities.

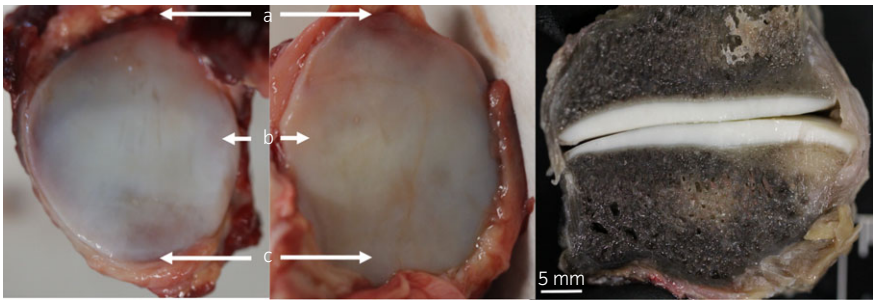

Fig 2: Gross morphological appearance of both the inferior (left) and superior (middle) facet articular surfaces, as well as the cross-section of the entire joint (right) following dissection and formalin fixation. The cranial, axial and caudal regions of the joint are highlighted using letters a, b and c. To ensure correct orientation was maintained throughout the collection process, ink was used to mark the fibrous capsule.

to apply a tare load of 0.98 mN to the tissue, and the tissue was allowed to reach tare creep equilibrium. A test load of 6.87 mN was then applied and the tissue was again allowed to reach creep equilibrium while the deformation was recorded over time. To achieve infinitesimal strain, a test load is selected that produces the least amount of strain (<10%). Once test equilibrium was reached, the test load was removed, and the tissue proceeded to recover. The maximum strain experienced by the tissue ranged between 2 and 11%. The compressive aggregate modulus, shear modulus and permeability of each sample were determined by fitting the creep deformation data using the linear biphasic theory [14].

Tensile testing

Samples were cut into dog bone shapes and photographed to measure width and thickness (Image J). In the superficial layer of the cartilage structure, collagen fibres are arranged parallel to the surface and are thought to increase the tensile properties in this region [15–17]. To assess the bulk properties of the cartilage, specimens with and without the superficial zone were tested. To remove the superficial zone, a specialised jig was created to remove 200 μm of cartilage from the surface with a cryotome blade. Either end of the sample was glued to paper tabs that were positioned a fixed distance apart; this distance was the gauge length and was always at least four times greater than the sample width. The paper tabs were clamped between the grips of a uniaxial test machine (TestResources[b]) and samples were then strained at a rate of 1% per second of the gauge length until failure. Using Matlab (MathWorks[c]), the resultant load vs. elongation curves were transformed to stress (normalised to the cross-sectional area) vs. strain curves. The linear region of the curve was used to determine the Young's modulus (Ey), and the maximum stress was considered the ultimate tensile strength (UTS) of the tissue prior to failure.

Biochemical analysis

Samples were lyophilised for 48 h and digested in 125 μg/mL papain (Sigma[a]) in 50 mmol/L phosphate buffer (pH = 6.5) containing 2 mmol/L *N*-acetyl cysteine (Sigma[a]) and 2 mmol/L EDTA (Sigma[a]) at 65°C for 18 h. Total sulfated GAG was quantified using the Blyscan Glycosaminoglycan Assay kit (Accurate Chemical[d]), based on 1,9-dimethylmethylene blue binding. DNA content was measured using the Quant-iT Picrogreen dsDNA Assay Kit (Invitrogen[e]). Finally, following hydrolysis with 2 N NaOH for 20 min at 110°C, the collagen content in samples was measured using a perchloric acid-free, chloramine-T-modified hydroxyproline assay [18] together with a Sircol collagen standard (Accurate Chemical[d]).

Histology

Following fixation, intact joints were rinsed several times in water and decalcified using 10% formic acid. Samples were then dehydrated, paraffin-embedded and sectioned at 6 μm. Sections were stained with haemotoxylin and eosin (H&E) for tissue architecture visualisation and safranin-O for GAG. In addition, picrosirius red was used to stain for all types of collagen and provided information on the organisation of collagen fibres and regional variances in content [19].

Data analysis

Statistical analysis was performed by a linear mixed-model ANOVA treating animal as a random effect. For biochemical and mechanical (compressive and tensile) results, the initial statistical model included inferior vs. superior surface, joint (i.e. C3–4, C4–5, etc.) and the interaction between surface and joint as fixed effects. For interpretation of tensile results, the presence or absence of the superficial zone was included as an additional fixed effect. Measurements obtained from the superior and inferior surfaces from C2I through C7S (C7I was not included) were averaged for results in which surface was not a statistically significant effect; A mixed-model ANOVA was repeated for the remaining effects. Significant differences among joints were assessed by Tukey's post hoc test when appropriate. Data are presented as mean ± s.d. and different letters denote significantly different groups at $P \leq 0.05$.

Results

Gross morphology and histology

Representative images of articulating surfaces of the equine cervical facet joint as well as a transverse section of this joint are shown in Figure 2. The opposing articulating surfaces were relatively flat, ovoid in shape and surrounded by a dense fibrous joint capsule. As there were no significant differences found between the average length, width and thickness of inferior and superior surfaces, the values were combined per level (Table 1). The average length was 41.36 ± 9.04 mm, 45.21 ± 13.42 mm, 53.14 ± 16.77 mm, 55.79 ± 16.81 mm and 55.97 ± 11.61 mm for levels C2/C3, C3/C4, C4/C5, C5/C6 and C6/C7 respectively (Fig 3). The average width was 38.58 ± 10.91 mm, 40.32 ± 10.26 mm, 46.38 ± 14.34 mm, 48.88 ± 18.12 mm, 48.27 ± 13.16 mm for levels C2/C3, C3/C4, C4/C5, C5/C6 and C6/C7 respectively (Fig 3). The average length and width did not

TABLE 1: Dimensions of inferior (I) and superior (S) facet joint surfaces at spinal levels C2 to C7. All values are presented as mean ± s.d.

Facet Surface	Thickness (mm)	Length (mm)	Width (mm)
C2I	1.74 ± 0.38	41.21 ± 9.42	35.21 ± 4.31
C3S	1.65 ± 0.40	41.51 ± 9.74	41.94 ± 16.09
C3I	1.55 ± 0.38	43.18 ± 14.09	40.03 ± 10.91
C4S	1.57 ± 0.35	47.24 ± 14.02	40.60 ± 10.84
C4I	1.68 ± 0.25	51.66 ± 18.31	46.19 ± 14.54
C5S	1.51 ± 0.44	54.62 ± 17.09	46.57 ± 15.85
C5I	1.84 ± 0.33	54.98 ± 17.83	48.44 ± 18.60
C6S	1.58 ± 0.50	56.60 ± 17.77	49.32 ± 19.78
C6I	1.62 ± 0.36	54.75 ± 11.83	48.23 ± 12.28
C7S	1.90 ± 0.46	57.19 ± 12.98	48.31 ± 16.14
C7I	1.67 ± 0.43	41.68 ± 16.96	41.60 ± 14.74

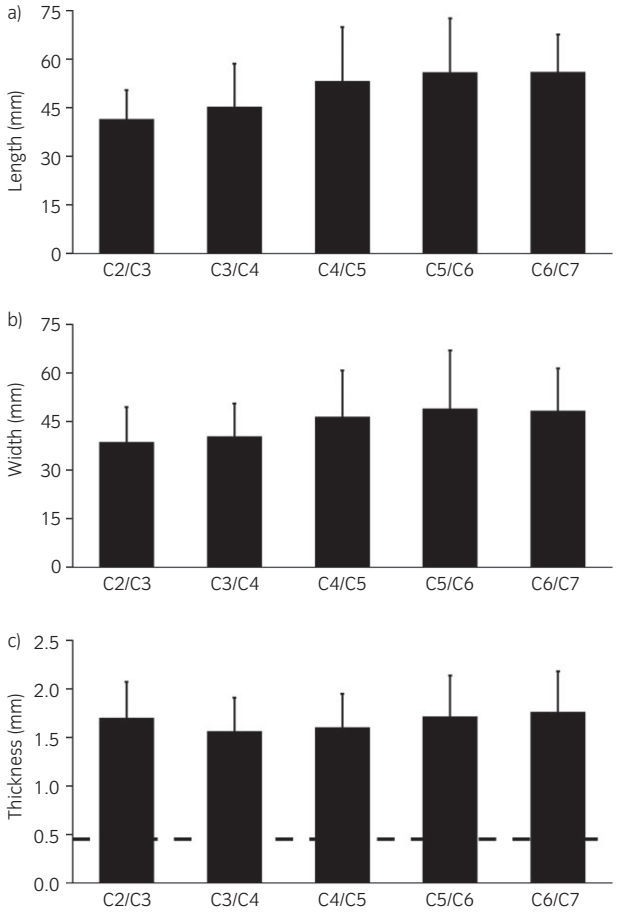

Fig 3: The average length (a), width (b) and thickness (c) of cervical facet cartilage found at each spinal level. Measurements of length, width and thickness were taken at the longest, widest and most central regions of the tissue, respectively and were not found to differ between joint surfaces and among spinal levels. For comparison, the historical value of the average thickness of equine carpal cartilage [24] is represented by a dashed line. All values are presented as mean ± s.d.

vary significantly among levels, although there was a trend for increasing width and length among C2/C3 and C5/C6, with C5/C6 being the largest level in terms of width and length. The average cartilage thickness for each level was measured to be 1.70 ± 0.37 mm, 1.56 ± 0.35 mm, 1.60 ± 0.35 mm, 1.71 ± 0.43 mm and 1.76 ± 0.42 mm for levels C2/C3, C3/C4, C4/C5, C5/C6 and C6/C7 respectively, with no significant differences among levels (Fig 3). It is important to note that measurements of thickness of the equine facet joint were taken at the site of testing and, therefore, may not be representative of the entire surface thickness. Dimensional data for each surface including C7 inferior are provided in Table 1.

H&E, picrosirius red and safranin-O stains of facet cartilage are presented in Figure 4. H&E staining revealed cells that were smaller and flatter in the superficial zone when compared with the intermediate and deep zones of the tissue. Furthermore, in the deep zone, cells were generally organised in a more columnar fashion. Samples had positive safranin-O staining for sulfated GAGs in the middle and deep zones; however, the stain was generally absent in the superficial zone. Safranin-O staining also highlighted the GAG-rich territorial and interterritorial matrix. In contrast to safranin-O, picrosirius red staining was most intense in the superficial zone. Overall, similar staining patterns and intensities were observed for the inferior and superior surfaces of each joint as well as among spinal levels.

Biochemistry

Comparing the GAG, collagen and cell content normalised to wet weight (WW) between opposing joint surfaces revealed no significant differences (Table 2). Additionally, the GAG/WW, collagen/WW and cells/WW were not statistically different among spinal levels (Fig 5). The average values of GAG/WW were 4.5 ± 1.1%, 4.0 ± 1.0%, 3.9 ± 1.0%, 4.4 ± 0.8% and 4.1 ± 0.9%, for spinal levels C2/C3, C3/C4, C4/C5, C5/C6 and C6/C7 respectively (Fig 5). The average values of collagen/WW were 13.2 ± 3.0%, 13.8 ± 2.6%, 13.1 ± 3.3%, 13.3 ± 2.4% and 12.5 ± 3.3% for spinal levels C2/C3, C3/C4, C4/C5, C5/C6 and C6/C7 respectively (Fig 5). Lastly, average cells/WW were 3618 ± 1159 cells/mg, 2359 ± 778 cells/mg, 2365 ± 1557 cells/mg, 3536 ± 1362 cells/mg and 3321 ± 1843 cells/mg for spinal levels C2/C3, C3/C4, C4/C5, C5/C6 and C6/C7 respectively (Fig 5).

Mechanical testing

Statistical analysis revealed no significant differences between the aggregate modulus, shear modulus and permeability of opposing inferior and superior joint surfaces (Table 3). Properties from opposing surfaces were averaged at each level and used for additional comparisons among spinal levels. The aggregate modulus, shear modulus and permeability values did not differ significantly among spinal levels. The average aggregate modulus, shear modulus and permeability values were 125.8 ± 56.9 kPa, 72.2 ± 32.6 kPa and 13.5 ± 14.1 × 10^{-15} m^4/Ns, respectively, for C2/C3; 133.1 ± 55.6 kPa, 75.7 ± 37.2 kPa and 19.8 ± 13.9 × 10^{-15} m^4/Ns for C3/C4; 103.3 ± 39.9 kPa, 60.7 ± 24.7 kPa and 20.0 ± 20.7 × 10^{-15} m^4/Ns for C4/C5; 121.6 ± 62.9 kPa, 73.6 ± 36.1 kPa and 20.2 ± 18.0 × 10^{-15} m^4/Ns for C5/C6; and 106.6 ± 36.5 kPa, 58.7 ± 21.4 kPa, 16.6 ± 11.1 × 10^{-15} m^4/Ns for C6/C7 (Fig 6a).

Young's modulus (Ey) and ultimate tensile strength (UTS) were measured for each surface from full-thickness samples as well as from samples with the superficial zone removed. Tensile properties for either group were not found to be significantly different between opposing inferior and superior joint surfaces (Table 3) and were therefore averaged at each spinal level. Ey and UTS values for full-thickness samples were, 5.3 ± 2.0 MPa and 4.1 ± 2.0 MPa for C2/C3, 4.3 ± 2.2 MPa and 2.4 ± 1.7 MPa for C3/C4, 5.6 ± 4.5 MPa and 3.5 ± 2.4 MPa for C4/C5, 6.1 ± 4.4 MPa and 4.4 ± 2.8 MPa for C5/C6, and 5.9 ± 3.2 MPa and 3.7 ± 1.8 MPa for C6/C7 respectively (Fig 6b). The Ey and UTS for samples with the superficial zone removed and averaged for each spinal level were 3.9 ± 2.5 MPa and 2.5 ± 1.1 MPa for C2/C3, 2.3 ± 2.0 MPa and 2.3 ± 1.9 MPa for C3/C4, 2.4 ± 1.9 MPa and 2.0 ± 1.0 MPa for C4/C5, 2.8 ± 2.2 MPa and 2.6 ± 1.9 MPa for C5/C6, and 1.4 ± 0.9 MPa and 1.4 ± 0.6 MPa for C6/C7 respectively (Fig 6b). In general, there was no significant difference among spinal levels for both Ey and UTS for both the full-thickness samples and samples with the superficial layer removed; however, the overall average Ey of full-thickness samples was significantly higher (denoted with letters in Fig 6b) than the overall average Ey of samples with superficial layer removed (5.4 ± 1.5 MPa vs. 2.6 ± 1.0 MPa respectively) and a similar finding was observed for the UTS (3.6 ± 1.0 MPa vs. 2.2 ± 0.6 MPa respectively).

Discussion

Despite the high prevalence of facet joint pathology in the equine cervical spine [5,6,11,20,21], this joint is understudied, and effective therapeutic options are largely lacking. Restoration of the articular surface via a tissue engineering strategy offers a potential solution for regeneration of damaged or malformed facet joint surfaces, but basic data regarding these tissues' properties, which would inform disease characterisation and provide therapeutic design criteria, are currently absent from the literature. The aim of this study was to characterise equine cervical facet cartilage in terms of both biochemical composition and biomechanical properties, in order to establish design criteria for potential cartilage repair products. The measured properties were compared with respect to spinal level as well as to joint surface (i.e. inferior vs. superior), using post-mortem tissue from six skeletally mature horses. Based on previous work describing articular

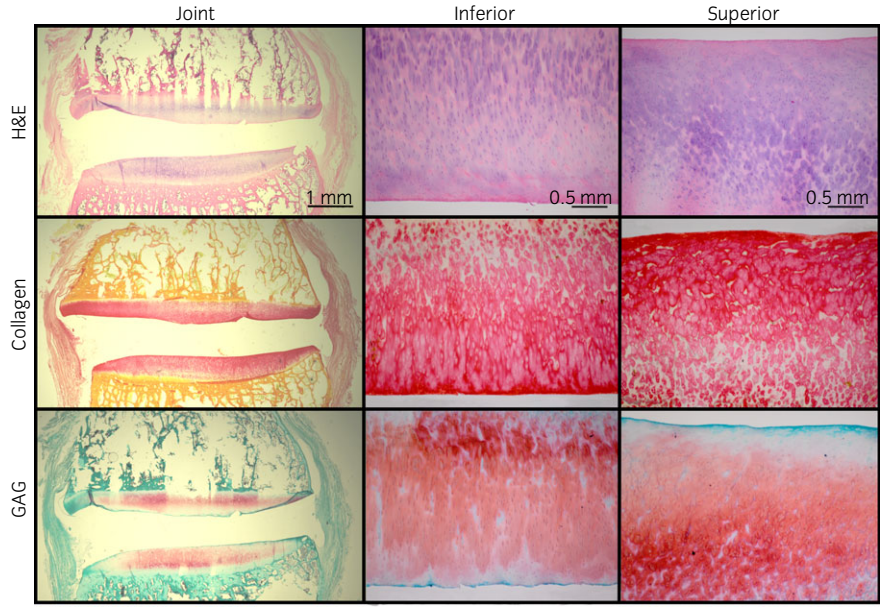

Fig 4: Representative cross-sectional photomicrographs of the entire facet joint (left) as well as the inferior (middle) and superior (right) surfaces of cervical facet cartilage. Histological stains H&E, picrosirius red and safranin-O reveal a typical articular cartilage structure that is rich in collagen and GAG.

cartilage properties of lumbar facet joints in multiple species, it was hypothesised that the properties of cervical facet cartilage would not differ significantly between opposing inferior and superior surfaces or across spinal levels [12]. Results demonstrated that biochemical and biomechanical properties were, indeed, similar between inferior and superior facet joint surfaces and, also, across spinal levels. One limitation of this study, however, is that measurements were taken from a single location per surface and do not provide a comprehensive topographic characterisation of this joint. This study provides the first comprehensive database of equine cervical facet joint cartilage properties, which will be useful for understanding both the aetiology of cervical facet joint degeneration and the development of new therapeutics, such as engineered grafts, for cervical facet cartilage repair.

With this characterisation study, it was demonstrated that the compressive properties of the equine cervical facet joint were substantially lower compared with that of other joints and facet cartilage of other species in spite of possessing comparable biochemical properties. The GAG and collagen contents on a per wet weight basis (3.9–4.5% GAG/WW and 12.5–13.8% collagen/WW) are comparable to those of equine articular cartilage found in other synovial joints as well as articular cartilage from the lumbar facet joints of other species (e.g. humans: 2.6% GAG/WW, 21.6% collagen/WW; mini pig: 4.2% GAG/WW, 15.8% collagen/WW; rabbit: 2.4% GAG/WW, 16.6% collagen/WW; canine: 3.8% GAG/WW, 16.8% collagen/WW)

TABLE 2: Biochemical properties of inferior (I) and superior (S) facet joint surfaces at spinal levels C2 to C7. All values are presented as mean ± s.d.

Facet Surface	Collagen/WW (%)	GAG/WW (%)	Cells/WW (cells/mg)
C2I	13.5 ± 3.4	4.3 ± 1.1	3170 ± 1090
C3S	12.9 ± 2.9	4.8 ± 1.0	4065 ± 1136
C3I	13.7 ± 2.5	3.6 ± 0.8	2190 ± 587
C4S	13.9 ± 2.8	4.4 ± 1.0	2528 ± 935
C4I	13.2 ± 1.9	4.1 ± 0.6	2742 ± 1959
C5S	13.0 ± 4.6	3.6 ± 1.2	1988 ± 1076
C5I	12.5 ± 1.6	4.4 ± 0.4	3714 ± 1163
C6S	14.1 ± 2.9	4.3 ± 1.1	3358 ± 1630
C6I	12.2 ± 3.9	4.1 ± 0.8	3855 ± 2058
C7S	12.8 ± 3.1	4.1 ± 1.1	2787 ± 1598
C7I	12.9 ± 2.0	3.9 ± 0.8	3172 ± 1803

[12,22]. Histologically, equine cervical facet cartilage resembles articular cartilage from that of other species and other equine synovial joints; the thickness of facet cartilage found in this study (1.6–1.8 mm) is comparable to those of the equine stifle joint (1.28–2.46 mm) [23] but quite different from that of the carpus (0.39–0.52 mm) [24]. The compressive stiffness of equine cervical facet cartilage was found to be substantially lower than articular cartilage from the equine stifle (unpublished data from our group) and from carpal joints (Fig 6a) [24]. In this study, the compressive aggregate modulus value of the cervical facet joint, averaged across all surfaces and levels, was 118 kPa, while a previous study found that the aggregate modulus of the equine carpus was over an order of magnitude higher, approximately 1290 kPa [24]. Similarly, shear modulus was higher in the carpus compared with the facet joint, 570 kPa in the carpus vs. 68 kPa in the facet, whereas permeability was lower, 3.5×10^{-15} m^4/Ns in the carpus vs. 18.0×10^{-15} m^4/Ns in the facet [24]. This phenomenon of low compressive properties compared with cartilage from other joints has been observed in facet cartilage of other species as well. For example, the aggregate modulus values in the rabbit and monkey (cynomolgus) have been reported to be approximately 600 and 700 kPa for the stifle cartilage, respectively [25], vs. an average of approximately 159 and 161 kPa for the lumbar facet cartilage respectively [12]. Based on the orientation of vertebral trabecular bone architecture in quadrupeds, it has been suggested that, in spite of horizontal orientation relative to the ground, quadruped spines are mainly loaded by axial compression. However, this loading is largely a function of ligaments and musculature, rather than gravity, as is the case for appendicular joints [26,27]. These findings suggest that, in general, the facet joint may be subjected to lower compressive loads in vivo compared with other joints.

Tensile properties of equine cervical facet cartilage were also low compared with articular cartilage of other equine joints. A study measuring the tensile modulus, or Ey, and the strength, or UTS, of stifle and fetlock cartilage found them to have an Ey of 6.3 and 15.5 MPa and a UTS of 9.9 and 10.3 MPa respectively [28]. In this study, the average Ey and UTS were found to be 5.4 and 3.4 MPa respectively. Not surprisingly, these properties were generally lower upon removal of the superficial zone, 2.4 and 2.1 MPa for Ey and UTS, suggesting that this zone plays an important role in the function of this tissue during tensile loading. Collagen fibres in the superficial zone are known to be arranged parallel to the joint surface [15], and this alignment is thought to contribute to the high tensile properties of this zone [15–17]. The superficial zone is only a small fraction of the total thickness of articular cartilage, however, and therefore is not an

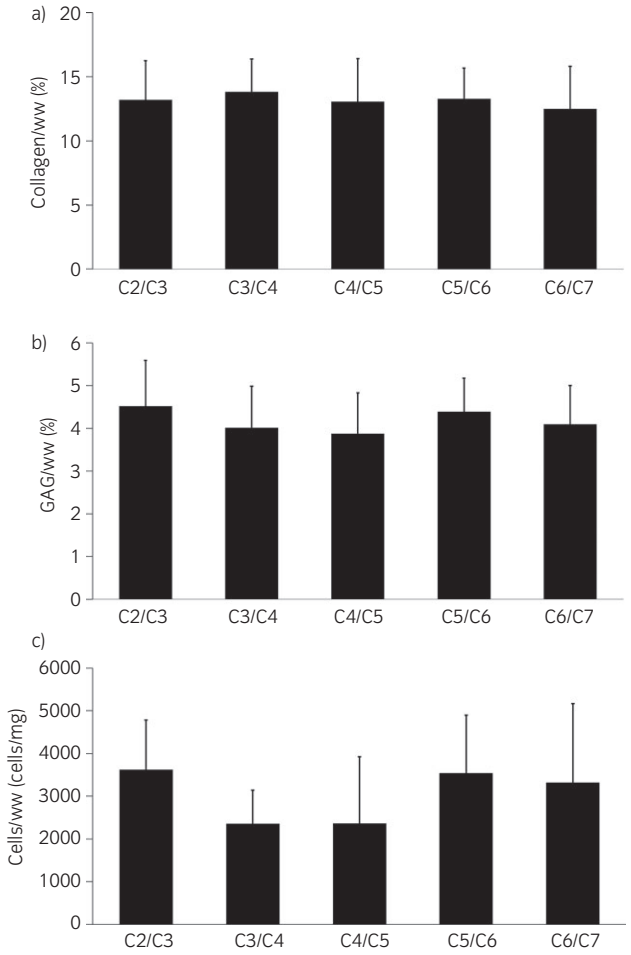

Fig 5: Average biochemical properties of equine cervical facet cartilage at each spinal level. Measurements of collagen/WW (a), GAG/WW (b) or cells/WW (c) were not found to differ among spinal levels. All values are presented as mean ± s.d.

accurate representation of the bulk of the tissue [29]. When developing strategies for cartilage repair, it is important to match the properties of the repair tissue with those of the surrounding native tissue to minimise stress concentrations and increase the chance of graft survival under physiological loading conditions [30,31]. Ideally, a repair tissue strategy could mimic the zonal architecture of native articular cartilage; however, given the limitations of current cartilage repair techniques, a more reasonable goal would be to match the bulk properties of the tissue. For this reason, we characterised the tensile properties with both the superficial zone intact as well as removed, to elucidate the properties of the bulk tissue underlying the superficial zone. Due to the relatively low tensile properties of the equine facet cartilage, a tissue engineering solution for cartilage repair may be more readily achievable for this joint.

The facet joints of the equine cervical spine are noted for their broad, flat surface area, facilitating the high range of flexion/extension (~21–35° per level) and lateral bending (~24–45° per level), and, to a lesser degree, axial rotation (~2–3° per level) [32]. The largest angular changes occur in the upper and lower cervical regions, while the mid-cervical segments move to a lesser degree [33,34]. Compressive forces are higher on the cranial aspect of the joint during extension and more on the caudal aspect of the joint during flexion [1], and joint moments created during flexion and extension are greatest in the caudal spinal segments [35]. Thus, it is somewhat surprising that properties of facet joint cartilage were not found to vary across spinal levels or between surfaces, given the variation in mobility across the cervical spine. Interestingly, the caudal cervical joints were found to be the most common location of osteoarthritis in adult horses [10]. The severity of cervical osteoarthritis has also been shown to correlate with the size of the horse [8]. Taken as a whole, the findings of this study that mechanical properties are low and do not vary among levels, despite large variations in mobility, and thus function, may explain the predisposition of certain levels to degeneration.

Radiographic changes consistent with facet osteoarthritis include joint space narrowing as a result of cartilage degeneration, the development of periarticular osteophytes or narrowing of the intervertebral foramina [5,6]. Although robust epidemiological data are lacking, caudal cervical facet osteoarthritis is considered a common finding in older horses [5,6,11,20,21]. It is thought that progressive bone changes are responsible for the decreased range of motion, nerve root impingement, lameness and pain associated with facet joint pathology [5,21]. However, in many cases, these bone changes are a secondary result of a primary cartilage lesion [36]. Therefore, treatment of articular cartilage lesions could preclude the onset of degenerative changes and may alleviate clinical signs associated with facet joint disease. This work provides a first step in developing effective therapies through the establishment of quantitative design criteria for engineered neocartilage for treating degenerative changes in the facet joint. Imaging modalities, such as CT, MRI and ultrasound, allow visualisation of bone quality and morphology [5], cartilage surface integrity [37], and synovitis and periarticular remodelling [38] respectively. These advanced modalities can be used upon localisation of potential lesions via a lameness exam and radiographs [5]. Ideal surgical candidates for cartilage repair could be those in early stages of osteoarthritis, as these joints may be more readily accessible due to less bone involvement.

TABLE 3: Mechanical properties of inferior (I) and superior (S) facet joint surfaces at spinal levels C2 to C7. All values are presented as mean ± s.d.

Facet Surface	Aggregate modulus (kPa)	Shear modulus (kPa)	Permeability $\times 10^{-15}$ (m^4/Ns)	Young's Modulus + Superficial (MPa)	Young's Modulus − Superficial (MPa)	Ultimate Tensile Strength + Superficial (MPa)	Ultimate Tensile Strength − Superficial (MPa)
C2I	92.3 ± 35.2	55.2 ± 21.3	16.7 ± 18.9	5.1 ± 2.4	5.2 ± 2.8	4.0 ± 1.6	3.2 ± 1.1
C3S	159.3 ± 26.5	89.2 ± 34.5	10.2 ± 7.3	5.5 ± 1.4	2.6 ± 1.2	4.2 ± 2.7	1.9 ± 0.7
C3I	112.3 ± 39.5	62.6 ± 27.3	21.7 ± 16.3	3.2 ± 1.2	2.5 ± 2.5	1.6 ± 0.5	1.7 ± 0.9
C4S	153.8 ± 64.9	88.8 ± 43.4	18.0 ± 12.4	5.3 ± 2.6	2.0 ± 1.4	3.3 ± 2.2	2.8 ± 2.5
C4I	106.2 ± 33.1	62.9 ± 20.7	24.8 ± 26.2	5.3 ± 4.3	2.1 ± 1.7	3.6 ± 2.2	1.8 ± 0.9
C5S	83.7 ± 61.2	48.7 ± 36.8	12.2 ± 10.2	5.9 ± 5.3	2.7 ± 2.1	3.3 ± 2.9	2.1 ± 1.2
C5I	124.3 ± 62.7	73.5 ± 36.8	25.9 ± 24.5	3.9 ± 3.4	3.0 ± 3.0	3.3 ± 2.1	2.9 ± 2.6
C6S	118.8 ± 68.9	73.8 ± 38.9	14.5 ± 6.3	8.2 ± 4.4	2.5 ± 1.4	5.5 ± 3.1	2.3 ± 0.8
C6I	126.8 ± 28.3	72.7 ± 15.6	13.0 ± 8.6	7.5 ± 3.5	1.4 ± 0.8	4.3 ± 2.0	1.5 ± 0.4
C7S	86.3 ± 34.0	44.8 ± 17.2	20.2 ± 13.4	4.2 ± 2.3	1.4 ± 1.2	3.0 ± 1.5	1.3 ± 0.8
C7I	108.8 ± 28.0	63.3 ± 19.1	18.2 ± 25.2	5.6 ± 3.4	2.5 ± 2.3	3.0 ± 1.5	2.3 ± 1.7

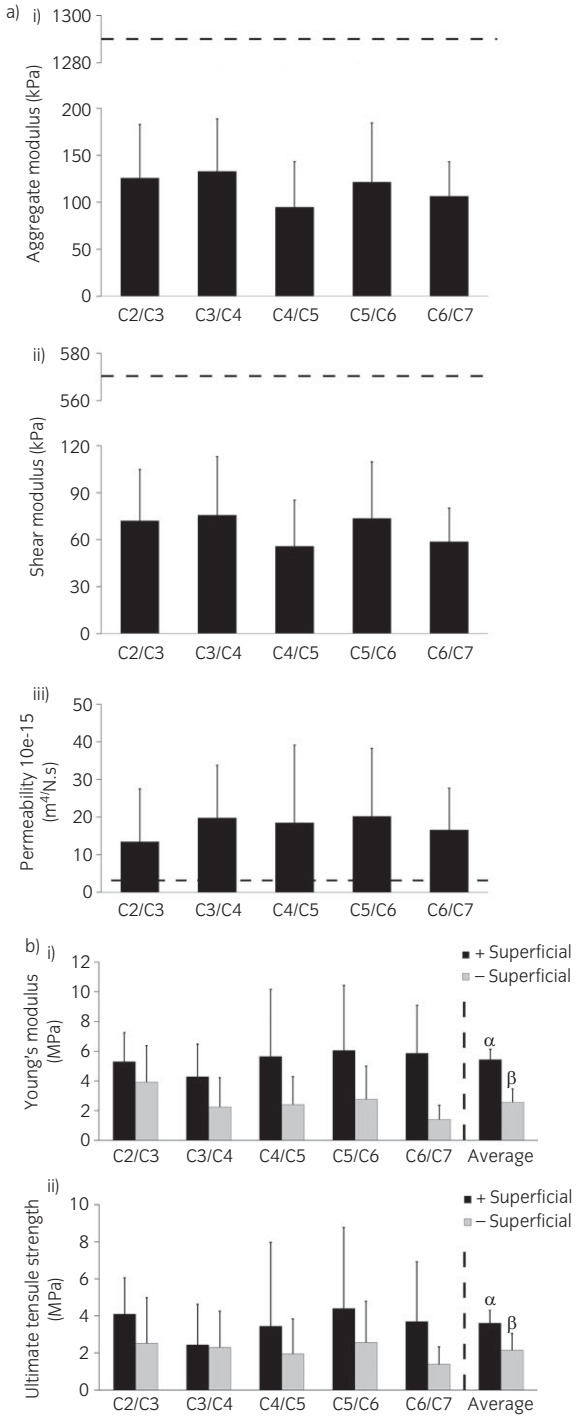

Fig 6: (a) Average biomechanical properties of equine cervical facet cartilage at each spinal level. The average aggregate modulus (i), shear modulus (ii) and permeability (iii) were not found to differ among spinal levels. Historical mean values of equine carpal cartilage aggregate modulus, shear modulus and permeability [24] are represented by dashed lines. All values are presented as mean ± s.d. (b) Tensile properties of equine cervical facet cartilage among spinal levels and between samples with superficial zone intact (black bars) and superficial zone removed (grey bars). The Young's modulus (i) and UTS (ii) did not differ among spinal levels. However, a two-way ANOVA revealed that average values of Young's modulus and UTS are higher for cartilage samples with a superficial zone compared with without (indicated by letters, α and β). All values are presented as mean ± s.d.

Given the relatively low mechanical properties as compared with articular cartilages of other joints, the facet joint's design criteria for an engineered cartilage replacement may be more easily attained than for other joints. Using a scaffoldless approach, self-assembled cartilage constructs have been formed with compressive aggregate modulus values ranging from 100 to 400 kPa [39–42], Ey values as high as 8.4 MPa and UTS values up to 3.3 MPa [43]. Self-assembled neocartilage has biochemical properties of 2–5% GAG/WW [39,41,42] and 15–20% collagen/WW [42], which are akin to those of the equine facet cartilage. Additionally, the facet joint has a small surface area in comparison to other synovial joints, making it more amenable to engineering a total surface replacement. This is important considering that cartilage-to-cartilage integration is a problem yet to be solved [44,45], and indeed, current strategies for human facet joint repair rely on a replacement strategy, such as the anatomic facet replacement system (AFRS) [46], total facet arthroplasty system (TFAS) [47] and total posterior arthroplasty prosthesis (TOPS) [48]. Another significant hurdle in the effort to generate an equine cartilage replacement strategy is the development of a minimally invasive surgical approach. Arthroscopic approaches have been used for other cartilage repair products [49]. When adhesives are required, gas arthroscopy is typically used. A minimally invasive technique for arthroscopic exploration of the equine facet joint was recently described, demonstrating that the full-joint surface is largely accessible arthroscopically [9]. Nevertheless, a surgical approach will have to be kept in mind during the engineering process in order to ensure ease-of-use and a minimally invasive strategy. It will undoubtedly be preferable to treat smaller lesions and at the earliest time point possible in order to minimise the amount of bone involvement. An osteoarthritic joint environment does not promote cartilage repair and would likely interfere with the integration of an implant [50]. The fact that current cartilage engineering protocols can yield biomimetic constructs with similar properties as native equine facet cartilage suggests that tissue engineering may offer a potential therapeutic strategy for treatment of cervical facet cartilage lesions. The discovery that properties do not differ significantly between opposing joint surfaces or among spinal levels reveals that site-specific replacements for cervical facet cartilage may not be necessary.

In conclusion, this investigation provides a comprehensive database of equine cervical facet joint cartilage properties. These results will augment our general understanding of this relatively understudied joint and can potentially aid in further studies of equine cervical spine biomechanics, such as development and validation of computational models, as well as tissue engineering strategies and establishment of the equine as a potential model for the human cervical facet. An appropriate animal model has yet to be established for the cervical spine, and therefore, the equine model could serve as the test bed for the development of current and future products for the treatment of facet related afflictions in humans. Overall, this work provides morphological, histological, biomechanical and biochemical data to facilitate development and design of novel treatment modalities for cervical facet lesions in horses.

Authors' declaration of interests

No competing interests have been declared.

Ethical animal research

Tissues were obtained from cadavers of client-owned horses that had been necropsied at the Veterinary Medical Teaching Hospital, University of California-Davis. The necropsy consent form signed by owners includes an option to opt out of research studies.

Sources of funding

This project was supported in part by funds provided by the National Center for Advancing Translational Sciences, National Institutes of Health, through grant number UL1 TR001860 and linked award TL1 TR001861. The

content is solely the responsibility of the authors and does not necessarily represent the official views of the NIH.

Acknowledgements

The authors would like to thank the owners that gave their consent to include their animals in this research study. The authors would also like to thank the staff at the Veterinary Medical Teaching Hospital, University of California, Davis for use of their necropsy facility.

Authorship

S. O'Leary and J. White contributed to study design and execution, and data analysis and interpretation. J. Hu and K. Athanasiou contributed to study design, and data analysis and interpretation. All authors contributed to the preparation of the manuscript and gave their final approval of the manuscript.

Manufacturers' addresses

[a]Sigma, St. Louis, Missouri, USA.
[b]TestResources, Shakopee, Minnesota, USA.
[c]MathWorks,Natick, Massachusetts, USA.
[d]Accurate Chemical, Westbury, New York, USA.
[e]Invitrogen, Carlsbad, California, USA.

References

1. Zsoldos, R.R. and Licka, T.F. (2015) The equine neck and its function during movement and locomotion. *Zoology* **118**, 364-376.
2. Dyson, S.J. 2011.Lesions of the equine neck resulting in lameness or poor performance. *Vet. Clin. N. Am.: Equine Pract.* **27**, 417-437.
3. Stewart, R.H., Reed, S.M. and Weisbrode, S.E. (1991) Frequency and severity of osteochondrosis in horses with cervical stenotic myelopathy. *Am. J. Vet. Res.* **52**, 873-879.
4. Mayhew, I.G., deLahunta, A., Whitlock, R.H., Krook, L. and Tasker, J.B. (1978) Spinal cord disease in the horse. *Cornell. Vet.* **68**, *Suppl.* **6**, 1-207.
5. Ross, M.W. and Dyson, S.J. (2010) *Diagnosis and Management of Lameness in the Horse*, Elsevier Health Sciences, Philadelphia, Pennsylvania.
6. Down, S.S. and Henson, F.M.D. (2010) Radiographic retrospective study of the caudal cervical articular process joints in the horse. *Equine Vet. J.* **41**, 518-524.
7. DeRouen, A., Spriet, M. and Aleman, M. (2016) Prevalence of anatomical variation of the sixth cervical vertebra and association with vertebral canal stenosis and articular process osteoarthritis in the horse. *Vet. Radiol. Ultrasound.* **57**, 253-258.
8. Rombach, N., Stubbs, N.C. and Clayton, H.M. (2014) Prevalence of osseous pathology in the articular process articulations in the equine cervical and cranial thoracic vertebrae. *Equine Vet. J.* **46**, *Suppl.* **47**, 10.
9. Pepe, M., Angelone, M., Gialletti, R., Nannarone, S. and Beccati, F. (2014) Arthroscopic anatomy of the equine cervical articular process joints. *Equine Vet. J.* **46**, 345-351.
10. Levine, J.M., Adam, E., MacKay, R.J., Walker, M.A., Frederick, J.D. and Cohen, N.D. (2007) Confirmed and presumptive cervical vertebral compressive myelopathy in older horses: a retrospective study (1992–2004). *J. Vet. Intern. Med.* **21**, 812-819.
11. Powers, B.E., Stashak, T.S., Nixon, A.J., Yovich, J.V. and Norrdin, R.W. (1986) Pathology of the vertebral column of horses with cervical static stenosis. *Vet. Pathol.* **23**, 392-399.
12. O'Leary, S.A., Link, J.M., Klineberg, E.O., Hu, J.C. and Athanasiou, K.A. 2017. Characterization of facet joint cartilage properties in the human and interspecies comparisons. *Acta Biomater.* **4**, 1-10.
13. Athanasiou, K.A., Agarwal, A. and Dzida, F.J. (1994) Comparative study of the intrinsic mechanical properties of the human acetabular and femoral head cartilage. *J. Orthop. Res.* **12**, 340-349.
14. Athanasiou, K.A., Agarwal, A., Muffoletto, A., Dzida, F.J., Constantinides, G. and Clem, M. (1995) Biomechanical properties of hip cartilage in experimental animal models. *Clin. Orthop. Relat. Res.* **316**, 254-266.
15. Benninghoff, A. (1925) Shape and construction of articular cartilage in its relationships to function. *J. Cell Res. Microscopic Anatomy* **2**, 783-862.
16. Helminen, H.J., Hyttinen, M.M., Lammi, M.J., Arokoski, J.P.A., Lapveteläinen, T., Jurvelin, J., Kiviranta, I. and Tammi, M.I. (2000) Regular joint loading in youth assists in the establishment and strengthening of the collagen network of articular cartilage and contributes to the prevention of osteoarthrosis later in life: a hypothesis. *J. Bone Miner. Metab.* **18**, 245-257.
17. Brama, P.A.J., Holopainen, J., van Weeren, P.R., Firth, E.C., Helminen, H.J. and Hyttinen, M.M. (2009) Effect of loading on the organization of the collagen fibril network in juvenile equine articular cartilage. *J. Orthop. Res.* **27**, 1226-1234.
18. Cissell, D.D., Link, J.M., Hu, J.C. and Athanasiou, K.A. (2017) A modified hydroxyproline assay based on hydrochloric acid in Ehrlich's solution accurately measures tissue collagen content. *Tissue Eng Part C. Methods* **23**, 243-250.
19. Montes, G.S. and Junqueira, L.C. (1991) The use of the Picrosirius-polarization method for the study of the biopathology of collagen. *Mem. Inst. Oswaldo Cruz* **86**, *Suppl.* **3**, 1-11.
20. Hahn, C.N., Handel, I., Green, S.L., Bronsvoort, M.B. and Mayhew, I.G. (2008) Assessment of the utility of using intra- and intervertebral minimum sagittal diameter ratios in the diagnosis of cervical vertebral malformation in horses. *Vet. Radiol. Ultrasound.* **49**, 1-6.
21. Nout, Y.S. and Reed, S.M. (2003) Cervical vertebral stenotic myelopathy. *Equine Vet. Educ.* **15**, 212-223.
22. Elder, B.D., Vigneswaran, K., Athanasiou, K.A. and Kim, D.H. (2009) Biomechanical, biochemical, and histological characterization of canine lumbar facet joint cartilage. *J. Neurosurg. Spine* **10**, 623-628.
23. Changoor, A., Hurtig, M.B., Runciman, R.J., Quesnel, A.J., Dickey, J.P. and Lowerison, M. (2006) Mapping of donor and recipient site properties for osteochondral graft reconstruction of subchondral cystic lesions in the equine stifle joint. *Equine Vet. J.* **38**, 330-336.
24. Murray, R.C., DeBowes, R.M., Gaughan, E.M., Mosier, D.E. and Athanasiou, K.A. (1995) Variations in the biomechanical properties of articular cartilage of the midcarpal joint of normal horses. *Vet. Comp. Orthop. Traumatol.* **8**, 11-18.
25. Athanasiou, K.A., Rosenwasser, M.P., Buckwalter, J.A., Malinin, T.I. and Mow, V.C. (1991) Interspecies comparisons of in situ intrinsic mechanical properties of distal femoral cartilage. *J. Orthop. Res.* **9**, 330-340.
26. Smit, T.H. (2014) The use of a quadruped as an in vivo model for the study of the spine – biomechanical considerations. *Eur. Spine J.* **11**, 137-144.
27. Sheng, S.-R., Wang, X.-Y., Xu, H.-Z., Zhu, G.-Q. and Zhou, Y.-F. (2009) Anatomy of large animal spines and its comparison to the human spine: a systematic review. *Eur. Spine J.* **19**, 46-56.
28. Lewis, C.W., Williamson, A.K., Chen, A.C., Bae, W.C., Temple, M.M., Wong, W.V., Nugent, G.E., James, S.P., Wheeler, D.L., Sah, R.L. and Kawcak, C.E. (2005) Evaluation of subchondral bone mineral density associated with articular cartilage structure and integrity in healthy equine joints with different functional demands. *Am. J. Vet. Res.* **66**, 1823-1829.
29. Athanasiou, K.A., Darling, E.M., Hu, J.C., DuRaine, G.D. and Reddi, A.H. (2017) *Articular Cartilage*, CRC Press, Boca Raton, Florida.
30. Nagel, T. and Kelly, D.J. (2013) The composition of engineered cartilage at the time of implantation determines the likelihood of regenerating tissue with a normal collagen architecture. *Tissue Eng. Part A* **19**, 824-833.
31. Khoshgoftar, M., Wilson, W., Ito, K. and van Donkelaar, C.C. (2012) The effect of tissue-engineered cartilage biomechanical and biochemical properties on its post-implantation mechanical behavior. *Biomech. Model. Mechanobiol.* **12**, 43-54.
32. Clayton, H.M. and Townsend, H. (1989) Kinematics of the cervical-spine of the adult horse. *Equine Vet. J.* **21**, 189-192.
33. Clayton, H.M., Kaiser, L.J., Lavagnino, M. and Stubbs, N.C. (2010) Dynamic mobilisations in cervical flexion: effects on intervertebral angulations. *Equine Vet. J.* **42**, 688-694.
34. Clayton, H.M., Kaiser, L.J., Lavagnino, M. and Stubbs, N.C. (2012) Evaluation of intersegmental vertebral motion during performance of dynamic mobilization exercises in cervical lateral bending in horses. *Am. J. Vet. Res.* **73**, 1153-1159.
35. Zsoldos, R.R., Groesel, M., Kotschwar, A., Kotschwar, A.B., Licka, T. and Peham, C. (2010) A preliminary modelling study on the equine cervical spine with inverse kinematics at walk. *Equine Vet. J.* **42**, 516-522.

36. Janes, J.G., Garrett, K.S., McQuerry, K.J., Waddell, S., Voor, M.J., Reed, S.M., Williams, N.M. and MacLeod, J.N. (2015) Cervical vertebral lesions in equine stenotic myelopathy. *Vet. Pathol.* **52**, 919-927.
37. Mitchell, C.W., Nykamp, S.G., Foster, R., Cruz, R. and Montieth, G. (2012) The use of magnetic resonance imaging in evaluating horses with spinal ataxia. *Vet. Radiol. Ultrasound.* **53**, 613-620.
38. Berg, L.C., Nielsen, J.V., Thoefner, M.B. and Thomsen, P.D. (2006) Ultrasonography of the equine cervical region: a descriptive study in eight horses. *Equine Vet. J.* **35**, 647-655.
39. Paschos, N.K., Makris, E.A., Hu, J.C. and Athanasiou, K.A. 2014.Topographic variations in biomechanical and biochemical properties in the ankle joint: an in vitro bovine study evaluating native and engineered cartilage. *Arthroscopy* **30**, 1317-1326.
40. Elder, B.D., Mohan, A. and Athanasiou, K.A. (2011) Beneficial effects of exogenous crosslinking agents on self-assembled tissue engineered cartilage construct biomechanical properties. *J. Mech. Med. Biol.* **11**, 433-443.
41. Makris, E.A., MacBarb, R.F., Responte, D.J., Hu, J.C. and Athanasiou, K.A. (2013) A copper sulfate and hydroxylysine treatment regimen for enhancing collagen cross-linking and biomechanical properties in engineered neocartilage. *FASEB J.* **27**, 2421-2430.
42. Natoli, R.M., Skaalure, S., Bijlani, S., Chen, K.X., Hu, J. and Athanasiou, K.A. (2010) Intracellular Na(+) and Ca(2 +) modulation increases the tensile properties of developing engineered articular cartilage. *Arthritis Rheum.* **62**, 1097-1107.
43. Lee, J.K., Huwe, L.W., Paschos, N., Aryaei, A., Gegg, C.A., Hu, J.C. and Athanasiou, K.A. (2017) Tension stimulation drives tissue formation in scaffold-free systems. *Nat. Mater.* **16**, 864-873.
44. Khan, I.M., Gilbert, S.J., Singhrao, S.K., Duance, V.C. and Archer, C.W. (2008) Cartilage integration: evaluation of the reasons for failure of integration during cartilage repair. a review. *Eur. Cell Mater.* **16**, 26-39.
45. Huey, D.J., Hu, J.C. and Athanasiou, K.A. (2012) Unlike bone, cartilage regeneration remains elusive. *Science* **338**, 917-921.
46. Goel, V.K., Mehta, A., Jangra, J., Falzan, A., Kiapour, A., Hoy, R.W. and Fauth, A.R. (2007) Anatomic Facet Replacement System (AFRS) restoration of lumbar segment mechanics to intact: a finite element study and in vitro cadaver investigation. *SAS J.* **1**, 46-54.
47. Zhu, Q., Larson, C.R., Sjovold, S.G., Rosler, D.M., Keynan, O., Wilson, D.R., Cripton, P.A. and Oxland, T.R. (2007) Biomechanical evaluation of the Total Facet Arthroplasty System (TM) - 3-Dimensional kinematics. *Spine* **32**, 55-62.
48. Wilke, H.-J., Schmidt, H., Werner, K., Schmoelz, W. and Drumm, J. (2006) Biomechanical evaluation of a new total posterior-element replacement system. *Spine* **31**, 2790-2796.
49. McIlwraith, C.W., Fortier, L.A., Frisbie, D.D. and Nixon, A.J. (2011) Equine models of articular cartilage repair. *Cartilage* **2**, 317-326.
50. Fahy, N., Farrell, E., Ritter, T., Ryan, A.E. and Murphy, J.M. (2015) Immune modulation to improve tissue engineering outcomes for cartilage repair in the osteoarthritic joint. *Tissue Eng. Part B Rev.* **21**, 55-66.